2013

Detection of Diffuse Seafloor Venting Using Structured Light Imaging

Clara J. Smart
University of Rhode Island, csmart@my.uri.edu

DETECTION OF DIFFUSE SEAFLOOR VENTING USING STRUCTURED LIGHT IMAGING

BY

CLARA J. SMART

A THESIS SUBMITTED IN PARTIAL FULFILLMENT OF THE

REQUIREMENTS FOR THE DEGREE OF

MASTER OF SCIENCE

IN

OCEAN ENGINEERING

UNIVERSITY OF RHODE ISLAND

2013

MASTER OF SCIENCE THESIS

OF

CLARA J. SMART

APPROVED:

Thesis Committee:

Major Professor Chris Roman

Harold T. Vincent

Steven Carey

Nasser H. Zawia

DEAN OF THE GRADUATE SCHOOL

UNIVERSITY OF RHODE ISLAND

2013

ABSTRACT

A systematic detection process capable of locating and quantifying diffuse seafloor venting using remote technology does not currently exist. Such venting is difficult to detect as it is characterized by both low temperature and low flux rates which cannot be distinguished using current remote acoustic or chemical sensors. Therefore the lack of understanding with regard to the distribution of active sites prevents a good estimation of the contribution of diffuse flow to thermal and chemical patterns within the broader ocean system.

Data collected over active vent fields have indicated that a structured light laser sensor, also used for high resolution seafloor bathymetric mapping, has the ability to detect near bottom temperature anomalies. Over areas of venting, changes in the index of refraction cause the projected laser line to appear blurred. To isolate and quantify this phenomenon image processing algorithms have been developed to detect diffuse venting using laser line images collected during near bottom surveys. This sensor system when mounted on an autonomous or remotely operated vehicle, will allow for large systematic surveys resulting in maps indicating areas of active venting. Analysis of multiple data sets indicates this system is capable of detecting both small point source vents and low temperature diffuse flow. Current analysis is qualitative with future quantitative goals being addressed in relation to the number of factors that contribute to the observed appearance of the laser line. Ultimately, the result of this research will be a map of vent activity over specific survey sites that can be quantitatively analyzed to provide an understanding of the extent and flux associated with diffuse flow sites.

ACKNOWLEDGMENTS

Many of those around me have allowed for the completion of this thesis.

The direction for this project comes directly from my advisor Chris Roman, who observed the first laser line distortions while surveying on the E/V Nautilus. While it may have seemed to be a data artifact at the time it has morphed, with his support and guidance, into a very exciting project. He has encouraged and assisted in the collection of data, contributed ideas and read many drafts of various papers.

Additionally, the community surrounding me within the lab is not only supportive but inspirational. Gabby was the original structured light laser pioneer whose calibration and stereo camera work has made my work possible. Ian's continual support for lab technology and improvement to the scripts required for map building are much appreciated and allow for forward progress.

I would also like to thank the field geologists whose constant support and encouragment this project keeps me going. Of particular note are Steve Carey and Chris German.

The collection of this data was made possible through research aboard the E/V *Nautilus*. Thank you to the ROV pilots who keep *Hercules* in the water, the crew of the ship and everyone else at IFE, ISC, and the Nautilus Program.

My mental and emotional state has remained mostly stable thanks to my friends and family, those near and far!

PREFACE

The following thesis has been prepared in manuscript format for submission to the journal Geochemistry, Geophysics and Geosystems (G^3). The goal of this paper is to introduce the structured light laser system as a sensor suite capable of systematic, remote detection of diffuse seafloor venting and small point source vents. Geologic justification is provided by Dr. Steven Carey. Three data sets collected in 2010 and 2011 illustrate the detection capability of this system as well as present interesting and complex detection problems. Continued work will isolate and address these detection anomalies. The structured light laser sensor is also under continuous development.

This manuscript has been prepared for submission to G^3 with the following title and author list.

Detection of diffuse seafloor venting using structured light imaging

Clara J. Smart, Chris N. Roman, Steven N. Carey

TABLE OF CONTENTS

Page

LIST OF FIGURES

Figure **Page**

Figure **Page**

MANUSCRIPT 1

Detection of diffuse seafloor venting using structured light imaging

by

Clara J. Smart [1], Chris N. Roman[2], Steven N. Carey [3]

In preparation for submission to Geochemistry, Geophysics, Geosystems (G^3)

[1]MS Student, Department of Ocean Engineering, The University of Rhode Island, Narragansett RI 02882. Email: csmart@my.uri.com

[2]Asst. Prof of Oceanography, Graduate School of Oceanography/Department of Ocean Engineering, The University of Rhode Island, Narragansett RI 02882. Email: cnr@gso.uri.edu

[3]Prof of Oceanography, Graduate School of Oceanography/Department of Ocean Engineering, The University of Rhode Island, Narragansett RI 02882. Email: scarey@gso.uri.edu

Abstract

Currently we lack a systematic and remote method for locating and quantifying diffuse sea floor venting using underwater robotic vehicles. Diffuse flow is characterized by both low temperature and low flux rates, which cannot readily be distinguished using current remote visual, acoustic, or vehicle-mounted environmental sensors. The result is a poor understanding of the distribution, contribution, and context of diffuse flow sources. An underwater structured light imaging system has however shown promise in detecting diffuse flows while completing sea floor imaging surveys at a typical altitude of 3m. The system creates sequential bathymetric profiles by imaging a laser line projected on the sea floor. In the presence of venting fluids, the laser line exhibits a detectable level of distortion due to variations in the refractive index along the optical path. By characterizing the degree of distortion it is possible to create maps of 'venting potential' with submeter spatial resolution. Results from three distinct vent fields are presented and discussed. Analysis of these data sets indicates this system is capable of detecting both small point source vents and low temperature diffuse flow.

1.1 Introduction

Fundamental questions exist regarding the role of diffuse fluid flow in the thermal and chemical exchange budgets of hydrothermal systems and cold seeps. However, due to the elusive nature of diffuse flow it cannot be systematically and remotely detected using current vehicle-mounted tools. While locations of larger point source vents can be determined through the use of acoustic and environmental sensors, understanding the spatial distribution of active diffuse sources within a vent field is elusive. The vehicle-mounted structured light laser system, originally developed for sub-centimeter bathymetric mapping, shows a sensitivity to index of refraction anomalies associated with active venting fluids during remote surveying

and has potential for better assessing this type of flow. This paper will discuss detection of diffuse seafloor venting using the structured light laser system beginning with an outline of the geologic value (Section 1.1.1) and an overview of the structured light system (Section 1.1.2). Section 1.2 will discuss existing vent detection methods while Section 1.3 will cover laser detection and survey methodology before Section 1.4 presents and discusses results.

1.1.1 Geologic Value

In hydrothermal systems fluid flow is typically classified as either vigorous high temperature focused flow, or low temperature diffuse flow. The latter is often found in low mounds and cracks frequently colonized by biological communities [1]. Diffuse flow within hydrothermal systems can represent a significant component of total fluid discharge ranging from 100% at some fields on the Galapagos spreading center [2] to 67% on parts of the Juan deFuca ridge [3] and can show high frequency temperature variability and activity over time [1, 4]. Additionally, from a chemical oceanographic perspective locating such venting may help identify areas rich in dissolved gasses such as methane and carbon dioxide which are often present in the diffuse venting at cold seeps.

Previous studies locating areas of diffuse flow and evaluating the heat and chemical flux through discrete measurements have interpolated findings over large areas of presumed active venting [5]. Due to the large surface area of diffuse venting, despite low flux rates, it has been estimated that the chemical and temperature contribution to the ocean system from diffuse venting is greater than the contribution from high temperature point sources or discrete venting [6] perhaps by a factor of five [7]. However, this cannot be verified without systematic detection and remote vehicle mounted mapping systems.

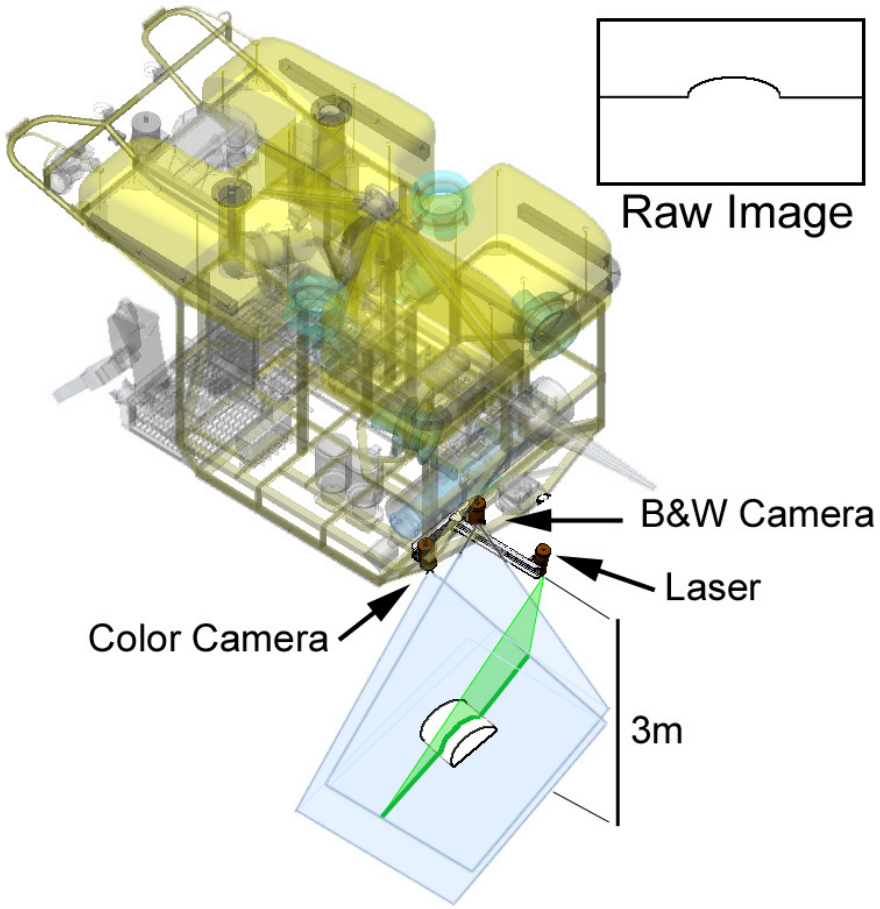

Figure 1: A CAD drawing of the *Hercules* ROV showing the structured light system's stereo camera and sheet laser locations. Each camera image captures a profile of the sea floor illuminated by the laser line (inset).

1.1.2 Structured Light Overview

The structured light laser system, shown mounted on the remotely operated vehicle (ROV) *Hercules* in Figure 1, was initially developed for sub-centimeter bathymetric mapping [8] and is a basic variant of several similar approaches [9–12]. Fundamentally, structured light imaging consists of a laser line projected onto a 3D surface and a camera to image that laser line. When viewed from the camera's perspective the line will follow the surface topography as if it was sliced along the laser plane. The structured light laser system consists of a stereo camera pair and an inclined 532nm green sheet laser mounted on a rigid frame with known relative geometry. Images of the projected laser sheet incident with the sea floor are recorded as the vehicle executes typical mow-the-lawn survey patterns. By

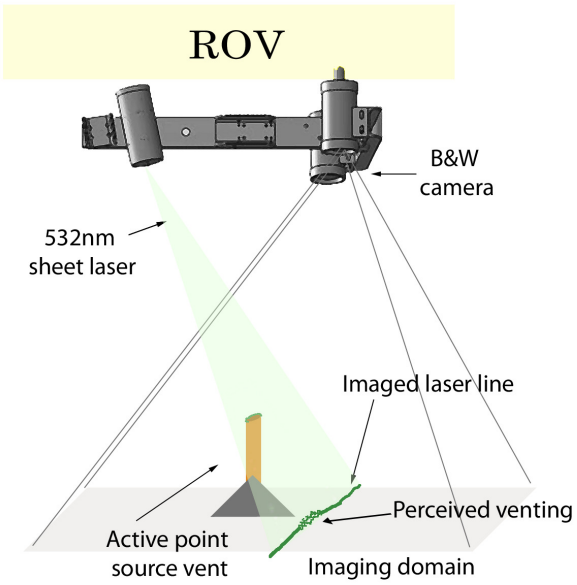

(a) Small point source vent

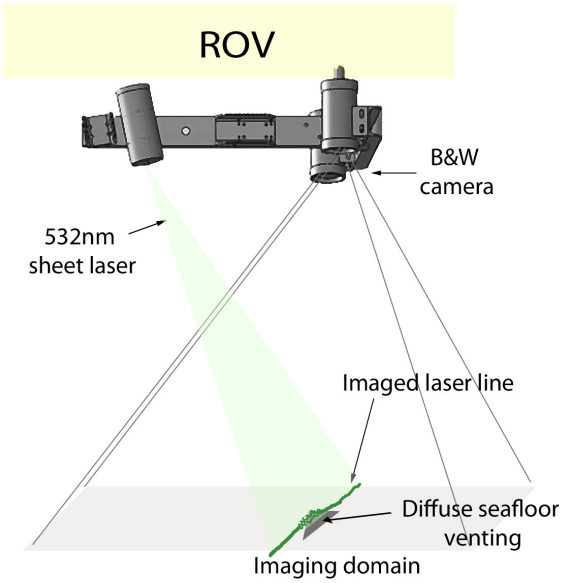

(b) Low level diffuse flow

Figure 2: Illustrations of laser line distortion as the sheet laser is refracted by different types of active venting. 2(a) While imaging small point source venting the laser disturbance is imaged on the sea floor beyond vent after interacting with the rising column of water. 2(b) The laser distortion is detectable directly at the diffuse vent source due to low flux rates.

detecting the vertical position of the laser line within a raw image, each capture can be converted to a single bathymetric profile analogous to a single ping of range data from a multibeam sonar. Bathymetry is established as each profile is reconstructed through triangulation given the appropriate calibration parameters. The system calibration is detailed in [13] and uses concepts from complete stereo calibration [14, 15].

While surveying active vent fields the sheet laser passes through venting fluids causing the laser line to refract due to index of refraction anomalies. The resulting a non-uniform laser line is imaged on the seafloor and indicates active venting along the ray path traveled by the sheet laser (Figure 3). As the laser sheet passes from the vehicle 3mabove the sea floor to the bottom, this distortion can be caused by high flux venting rising meters above the seafloor as well as low flux venting undetectable centimeters above the bottom. While surveying small high flux point source vents the laser sheet intersects the column of venting fluid above the bottom and is projected beyond the vent (as a function of the laser sheet angle) before being imaged on the sea floor (Figure 2(a)). As the vehicle travels over a vent the observed distortion will continue behind the vent until it is undetectable. Laser line distortion indicates a change in the index of refraction along that ray, not necessarily at the point on the seafloor where the laser line is imaged. In the case of low flux, low temperature venting, which mixes quickly, the laser line tends to be distorted and imaged at the source of venting (Figure 2(b)). While some spatial resolution is lost, active point source venting can still be determined to sub-meter accuracy and the source of diffuse venting can be located to within tens of centimeters.

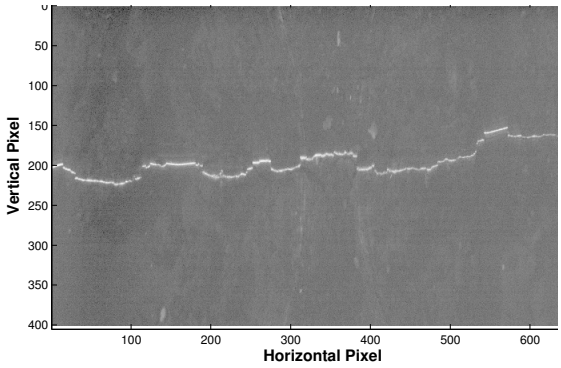

(a)

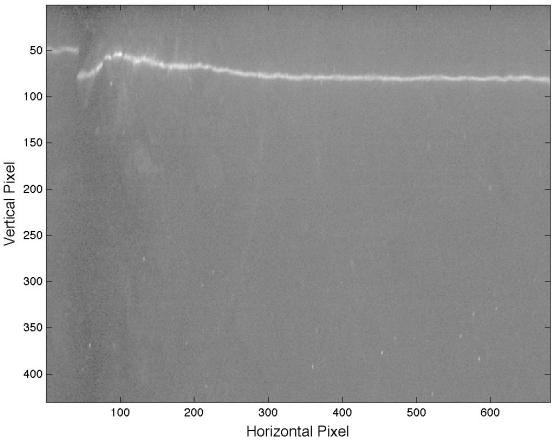

(b)

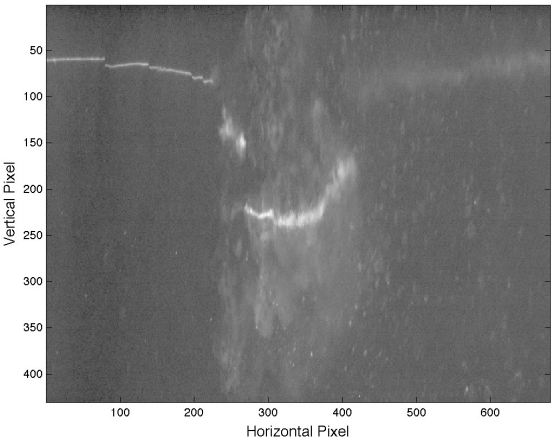

(c)

Figure 3: The laser line becomes refracted as it passes over venting fluids with altering the index of refraction of sea water. 3(a) Shows a crisp laser line over a geological site with no venting present. 3(b) Reveals slight distortion in the laser line as low temperature or low flux flow is surveyed. 3(c) Presents an example of the laser passing over an active small point source vent with significantly higher temperature and flux rates.

1.2 Review of Existing Vent Detection Methods

As previously described, diffuse venting is difficult to map due to near ambient temperatures and low flux rates and bottom mixing. Robust diffuse vent detection processes capable of completing systematic surveys remotely over areas on the order of square kilometers in size are currently inefficient and inconsistent. Potentially observable temperature and chemical signals decay rapidly due to mixing and are no longer detectable just meters above the sea floor. In most cases, diffuse vent sites are found as a secondary consideration following the localization and exploration of larger point source vents using towed or autonomous underwater vehicle (AUV) systems operated 50-400m above the sea floor [16]. More detailed low altitude ROV or AUV surveys will typically identify areas of biological activity associated with venting, rather than the venting itself [17, 18]. For these reasons, the full extent and the distribution of a diffuse vent field is rarely determined, and the entire process is likely to miss vent fields consisting of only diffuse flow sources [1].

Specific approaches to identify active venting have been developed using both visual and acoustic methods. The ultimate goal following detection is the ability to provide quantitative data regarding the temperature and flux of the venting source.

1.2.1 Point Source Vent Detection

The most successful vent detection schemes, which focus on point source vents, require an AUV or ROV, fitted with various sensors to detect anomalies in magnetics, chemistry and temperature to complete multiple surveys to isolate the center of the plume [16]. For example, an initial a pre-determined survey is completed 100-400mabove the seafloor searching for anomalies indicative of buoyant plumes. Fundamentally, this processes will only localize high temperature high flux venting which creates observable high altitude buoyant plumes. Assuming a potential

plume is detected, a second higher resolution survey is completed at an altitude of 50mto isolate the center of the vent source. Finally, a third survey employing either a manned submersible, AUV or ROV completes detailed imaging, flow and temperature analysis of both the point source vent and the surrounding area [17]. Therefore, only diffuse venting surrounding the large point source vent may be identified. Hence, this method favors the detection of point source, high flux or high temperature vent systems, and frequently may not locate vent fields containing only diffuse venting as discussed by [1].

Furthermore, three-dimensional acoustic maps of active black and white smokers have provided volumetric and flow analysis [19]. The Cabled Observatory Vent Imaging Sonar (COVIS) [20], a multibeam sonar and rotatory system installed at the Main Endeavor Field (MEF) on the Juan de Fuca Ridge computes 3-D plume maps through detection of backscatter due to suspended particulates and strong temperature gradients. As this method primialry focuses on point source venting, only diffuse flow located on the structure being imaged may be detected through acoustic scintillation, which provides only a broad understanding of its presence.

1.2.2 Diffuse Vent Detection

Visually, diffuse flow can be detected by watching an ROV-mounted high definition video feed for "shimmering water" (Figure 4) [21]. The shimmer or mirage effect indicates change in the index of refraction which is predominately caused by increased water temperature relative to ambient but is influenced by salinity and turbulence [22]. However, this phenomena is only visible on the order of centimeters above the seafloor and is primarily detected in situ with the human eye through the use of high quality video with fast frame rates. Diffuse venting is often clear with few particulates causing the presence of this mirage to be the only visual marker. The required near bottom observations and time consuming obser-

Figure 4: Visually identifying diffuse venting requires finding 'shimmering water' with a high quality video system. A still image makes this property difficult to identify, as demonstrated by the shimmer present in the top right and center left of this image taken at the Kolumbo crater, *ROV Hercules, E/V Nautilus*.

vation based detailed approach makes this technique inefficient and unsystematic for detection of diffuse vent fields. However, it can be used to determine areas to physically sample.

Experiments recreating this anomaly produce Schlieren-like flows allowing for the visualization of density fluctuations in controlled lab settings. With sufficiently defined parameters a quantitative description of a particular flow and the index of refraction can be made [23, 24]. In real situations additional factors, such as the presence of dissolved gases (eg. CO_2 or CH_4), fluid composition and turbulence due to bottom mixing will also have an affect complicating any estimates.

A series of acoustic diffuse vent detection methods started with detection of uncorrelated acoustic backscatter using a 330kHz Mesotech sonar system mounted on the DSV *SeaCliff* [25]. This conical beam sonar scanned parallel to the sea floor intercepting rising near bottom diffuse flow. Venting can be detected through the analysis of uncorrelated returns caused by the temperature-dependent changes in acoustic impedance. During data collection the vehicle remained stationary and

was positioned to minimize sea floor obstructions in the sonar's view. Additional acoustic detection approaches include computing temperature based of the speed of sound as determined by the difference between returns emitted from a stationary sonar system [26]. The stationary nature of these approaches do not allow for the systematic surveying and exploration of large vent fields.

1.2.3 Flux and Temperature

Once diffuse flow is located, quantitative measurements are necessary to increase the scientific understanding of the vent field. Ideally, a complete survey would show locations with estimated temperature and flux of diffuse flow. The most direct approach for establishing temperature requires an array of temperature probes distributed across an active diffuse vent field [1, 4] or manipulated temperature probes and direct flow meters [6, 27]. Such tactile and sampling approaches are good for small areas, but don't translate well to organized surveying or prospecting in new locations.

Visual quantification of flux has been approached using diffuse flow velocimetry (DFV) which detects and tracks refractive anomalies as they pass in front of a stationary background [28]. This approach was evaluated at the Lucky Strike Vent Field based on collected high speed video segments, temperature probe measurements, and geo-referencing with image mosaics [29, 30]. This solution requires isolation of a small volume of fluid and does not immediately lend itself to systematic surveys with a moving platform.

The previously introduced COVIS system, mounted on the Endeavor node of the NEPTUNE project, monitors the output of several point source vents and the discharge rates of diffuse flow in the surrounding area. The diffuse flow is measured using scintillation, which looks at fluctuations in the acoustic return caused by turbulence, to estimate flow in a direction perpendicular to the acoustic path [19].

The flow estimates are then translated to a measure of flux and evaluated for time varying changes [20]. These methods, although successful, do not translate easily to surveys from a moving platform. Vehicle motion will complicate the measurements and the horizontal observation direction is not conducive to high spatial collocation with other data products (multibeam and images) collected in a down looking manner.

1.3 Laser Detection Methods

1.3.1 Signal Detection

The index of refraction of seawater is altered by changes in pressure, temperature, wavelength and salinity. For the purposes of this study pressure and wavelength (532nm) are constant. Venting fluids have consistently higher than ambient temperature while salinity can greatly vary within a plume due to density driven mixing. Values for the index of refraction as a function of temperature (up to 40°C), pressure, wavelength and salinity are presented in [22] as an empirical 27 term equation. The index of refraction for higher temperature seawater is discussed in [31]. Additionally, the varied chemical composition of the venting fluids will cause the index of refraction to differ slightly from the analytically computed values. The visual affect of small changes in the index of refraction are directly illustrated by schlieren type experiments [32].

Turbulence caused by the flux of venting fluids and bottom currents creates an inhomogeneous medium with spatially varying index of refraction. The concept of a real index of refraction and the effect of turbulence is introduced by [33]. Turbulent blobs cause continuous angular deviation of light rays leading to additional small changes in the index of refraction increasing the scattering region (θ_s). Maximum increases to the scattering angle occur with increasing salinity and temperature in the presence of turbulence. It is also noted by [33] this effect can significantly

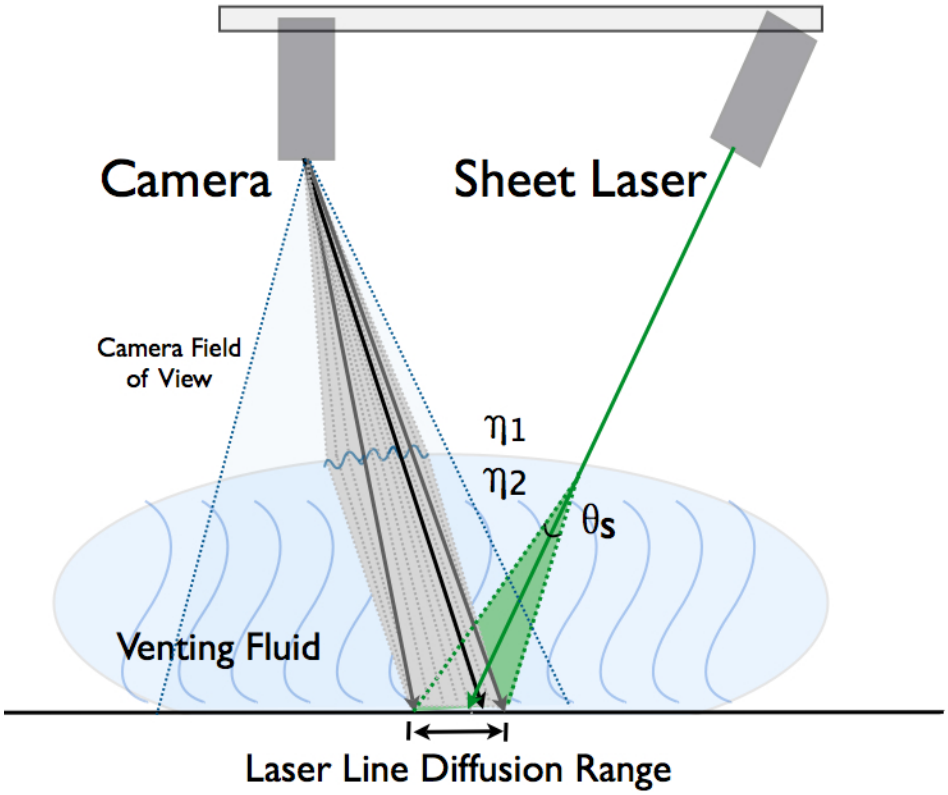

Figure 5: In the presence of active venting the sheet laser passes from the vehicle through media with varying refraction index due to temperature, salinity and turbulence which increases the scattering angle of the light. As the laser line is captured by the camera it is also altered by changing media, further increasing the scattering angle and resulting in an image of a blurred laser line.

degrade image quality, which is observed as the laser line is no longer clear and crisp in the presence of active venting.

The optical path of the laser will pass through the venting fluids with a range of optical and turbulent properties before reaching the seafloor, and again pass through on the path to the camera, effectively doubling the impact of the scattering angle (Figure 5). The resulting blurred laser line image is the net result of the laser line scattering within this envelope.

By imaging the laser line in this scenario active venting can be determined and spatially identified. Sample images showing varying degrees of venting are shown in Figure 3. Our approach thus far has been to compute intensity weighted statistical moments about the peak of the laser line in each image column. This characterizes the amount of laser spread and can be used as a proxy for 'venting potential' [34]. A weighted second moment about the peak of the laser line v^* over a vertical window of size w in each column as illustrated in Figures 6 and calculated using

$$\sum_{i=v^*-\frac{w}{2}}^{v^*+\frac{w}{2}} r_i(v_i - v^*)^2. \tag{1}$$

Here v_i and r_i are the comparison pixel location intensity respectively.

Laser profiles including a larger a scattering envelope due to venting will have a greater second moment and therefore a higher venting potential based on this computation (Figure 7). Examples of laser line cross sections showing varying degrees of spreading are shown in Figure 9.

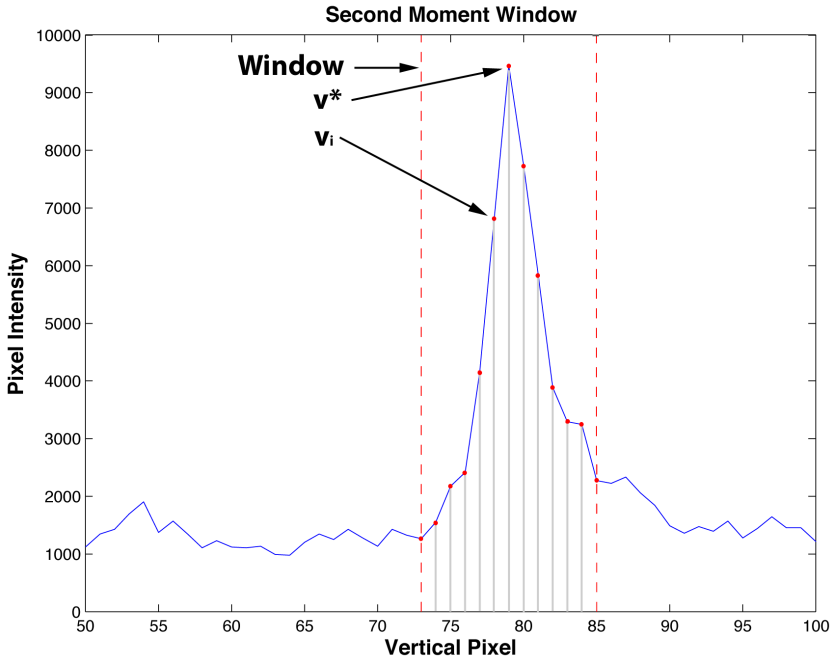

Figure 6: Cross section of the laser line annotated to compute the weighted second moment about the centroid of the line.

1.3.2 Laser Line Extraction

Data acquisition (further discussed in Section 1.3.3) and detection of the laser line through image segmentation processes are identical to the bathymetric approach [13]. However, unlike the bathymetric approach, the peak of the laser line is necessary for the weighted second moment computation of venting potential. The steps of the laser extraction batch processing algorithm are outlined below in detail, with steps 1-4 common to both bathymetric surveys and vent detection. The initial raw images are 12bit black and white photos of the laser line incident with the seafloor.

1. A binary mask is created by thresholding the 12bit image of the laser line (Figure 8(b)). The intensity threshold is determined by a Neyman-Pearson test where the signal (the laser line) is deterministic and all background intensity values are considered noise. Altering the desired value of the prob-

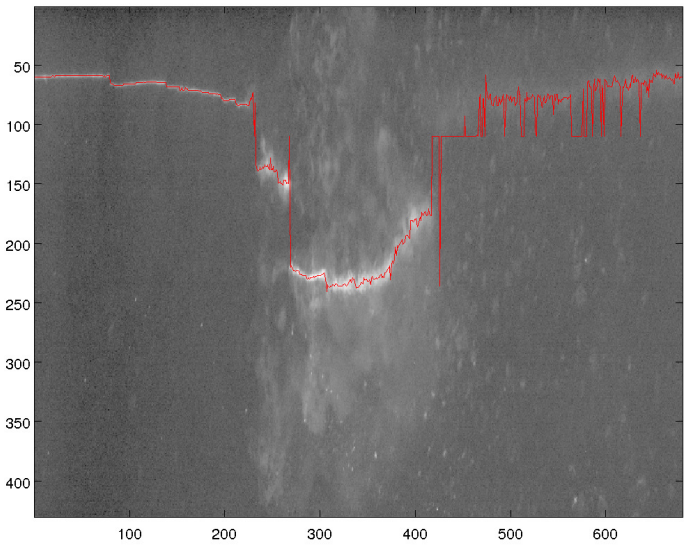

(a)

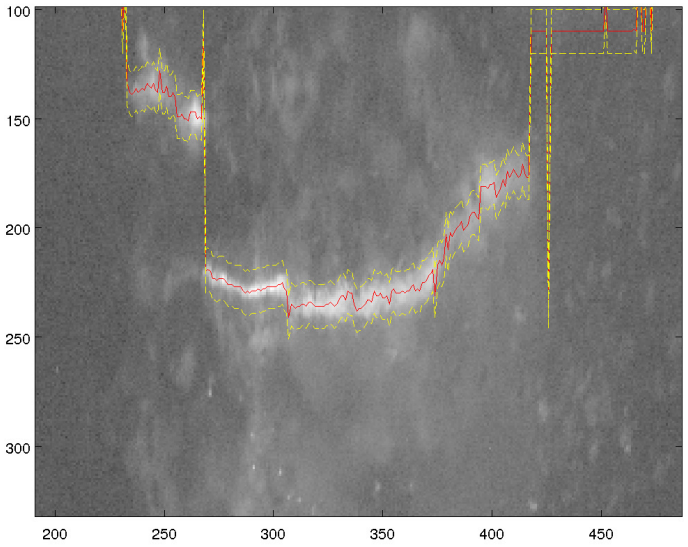

(b)

Figure 7: Computing the second moment about the laser line location. 7(a) Center of the laser line (red) is identified using extraction algorithms. 7(b) Zoomed in view of the laser line illustrating a the window (yellow) about the extrated line within which the second moment is computed. (The logrithmic image is shown for clarity.)

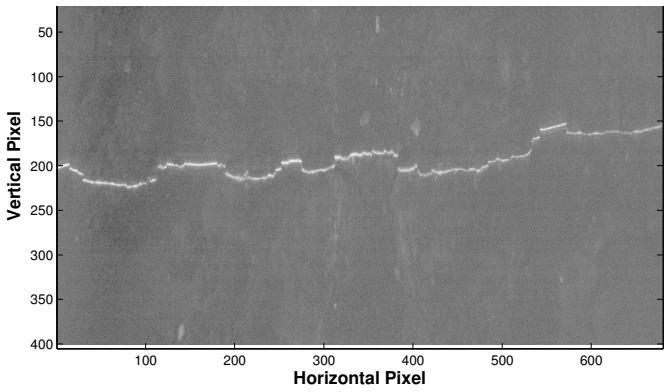

(a) Log image of the laser line

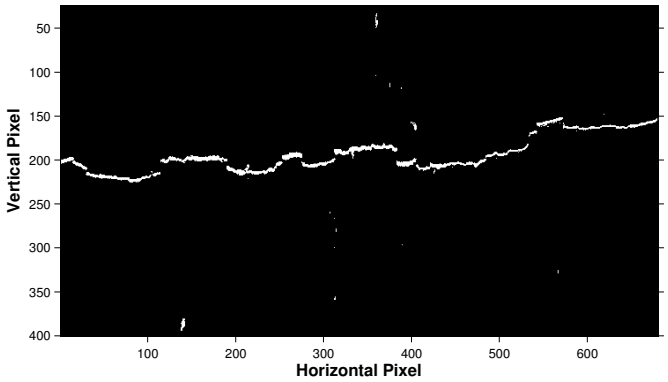

(b) Initial threshold mask

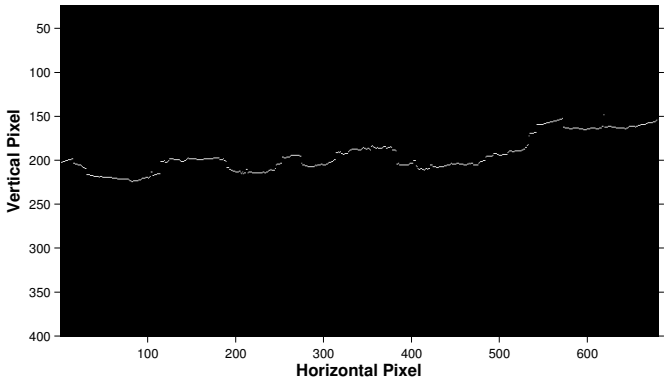

(c) Final laser line extraction

Figure 8: The laser extraction via image segmentation processes. 8(a) An image of the laser line over the sea floor. 8(b) thresholded image highlighting the selected pixels. 8(c) The location of the laser line centered peak as a single value in each image column v.

ability of a Type I error (probability of false alarm) adjusts the threshold level.

2. Each column within the image is then processed and viewed as an independent 1D signal containing the cross-section of the laser line. The peak intensity of the laser line is at an unknown location v^*. At this point any pixel having an intensity value greater than the previously determined threshold is a possible element of the laser line cross-section.

3. Each image column may contain multiple clusters of contiguous pixels above the threshold. The cluster locations are then compared to the median laser line location found in neighboring columns and their sizes are compared with the median line width across the entire image. In the absence of venting this is typically 1-3 pixels and varies with bottom type, water clarity and survey altitude. The cluster with properties closest to both medians is selected as the laser line.

4. For each column, the pixel of maximum intensity within the selected cluster is chosen as the center of the line and denoted v^*. The resulting pixels create the laser line profile (Figure 8(c)).

5. With v^* identified the 'venting potential' as described in Section 1.3.1 is calculated for each image column.

This algorithm is set up as a batch process which produces a complete set of laser line profiles each with the calculated venting potential. The profiles can be correlated with the vehicle's navigation data to create a complete map showing the spatial distribution of active venting at a survey site.

To complete a map of venting potential no additional tools or procedures are necessary during data acquisition. The same laser images can be used to create

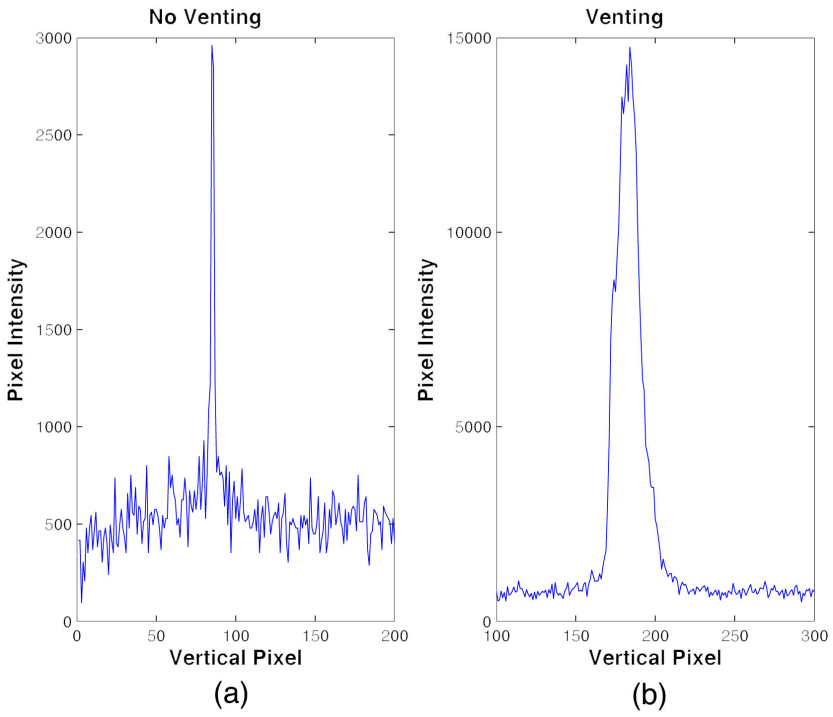

Figure 9: Comparison between laser line cross sections. (a) An image over plain seafloor showing a typical 1-3 above threshold pixel spread. (b) An image over a high flux point source vent. Both cross sections are shown over the same horizontal scale.

both spatially co-located bathymetric maps and vent maps. Furthermore, the laser images are collected simultaneously with still images used for photomosaics (such as Figure 16(a)) and high resolution multibeam bathymetry.

1.3.3 Survey Methodology

The structured light system set-up discussed in this paper consists of two Prosilica GC1380 cameras and a 100mW 532nm green sheet laser manufactured by Diode Laser Concepts, Inc. The stereo cameras are mounted in 6000m rated pressure housings and arranged in a 300mm baseline stereo configuration. The laser, in a 6000m housing, is mounted 600mm from the camera baseline and is verged to intersect the camera optical axes at a range of 3m, the typical survey altitude. This arrangement translates to a range resolution of 0.5cm per camera pixel. The sensor rig is mounted at the back of the vehicle away from the forward operational lights to ensure the image background is as dark as possible and improve the signal to noise ratio.

The survey data analyzed in this paper was collected using the vehicle platform Hercules, a Remotely Operated Vehicle (ROV) shown in Figure 1. This 4000m rated ROV is closed loop controlled and completes organized trackline surveys at prescribed velocities and altitudes. The navigation sensor suite includes a 600kHz RDI Doppler velocity log (DVL), a Paroscientific pressure depth sensor and an OCTANS fiber optic gyro system for heading and attitude information. These data are collected using the DVLNAV software package [35].

During a high resolution imaging survey the vehicle is typically flown at speeds of 15 to 25cm/s and a constant altitude between 2 and 4m off the bottom. The laser line is imaged at approximately 20Hz, creating a survey resolution better than one laser line per centimeter along track and 2-4 laser points per centimeter across track. A standard high resolution survey 30 x 30m in size and can be

completed in about 30 minutes. This sensor system is well understood and has been used to collect data for high resolution maps of geological and archaeological sites [8, 13, 36, 37].

1.4 Results and Discussion

Our first observation of a blurred laser line due to refraction occured during a 2010 survey in the active Kolumbo Submarine Volcano Crater near Santorini, Greece [21, 38, 39]. This led to the development of the current vent detection algorithm. This process was then applied to additional surveys completed during 2010 and 2011 over known vent fields with the Kolumbo Crater and at the Palinuro Seamount, Italy. [40]. An overview of the resulting maps of venting potential follows.

1.4.1 Kolumbo Vent Field, 2010

The Kolumbo Submarine Volcano is the largest volcano of the Kolumbo Volcanic Rift Zone and last erupted in 1650CE. The crater is approximately 3km in diameter with a maximum depth of 500m [21, 38]. This area is characterized by numerous chimney structures up to three meters high, CO_2 bubbling, and venting fluid with reaching temperatures 200°C above ambient (Figure 10). Temperature probe measurements and high definition (HD) video taken during numerous ROV dives within the area confirm our initial vent detection results.

The ROV surveyed 3m above the seafloor capturing structured light images as discussed in Section 1.3.3. Blurring and distortion of the laser line was apparent in the raw black and white images as the laser line was imaged over known active vents. A map depicting venting potential within a section of the main vent field is shown in Figure 11(a). For a better understating of vent field activity within the area, the corresponding map of laser bathymetery is shown in Figure 11(b).

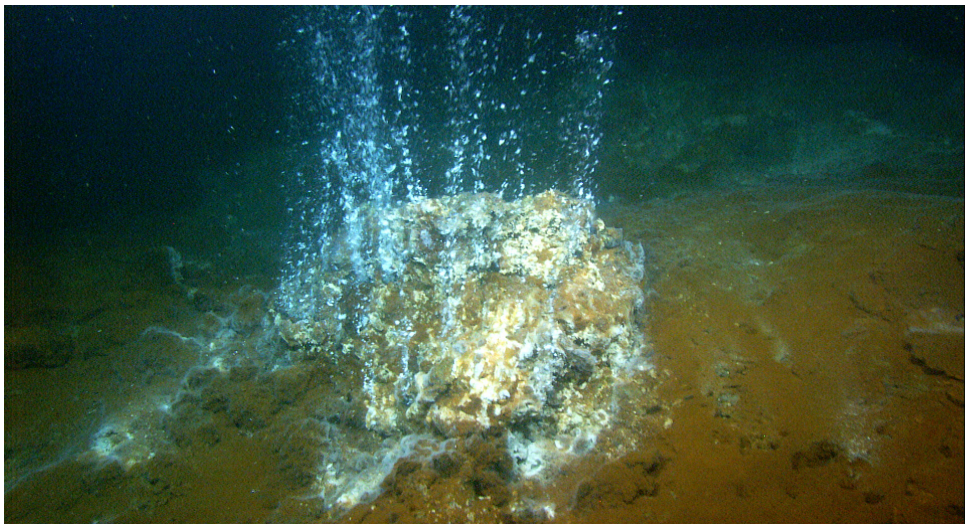

Figure 10: An active vent within the Kolumbo Crater off the coast of Santorini, Greece. This vent field contains diffuse and small point source vents with temperatures reaching 200C above ambient.

Comparison between the two maps indicates the currently active hydrothermal vent structures and additional areas of diffuse seafloor flow. For example, the tall structure marked A is an active vent. The significant laser line refraction indicates high temperature venting most likely accompanied by high flux and turbulence. Additionally, areas appearing to be flat seafloor in the bathymetric maps, such as that marked B, contain diffuse flow as detected by the structured light laser system and confirmed with the ROV and HD video.

Isolated vent within the Kolumbo Crater

The majority of the active vents with in the main vent field of the Kolumbo Crater are small point source vents. High definition videos of shimmering water flowing from the vent provides visual confirmation of active venting moments before the laser line images are captured (Figure 12). Focusing on a single active spire it is possible to discern the sources of active flow within the structure relative to the spires. he resulting vent detection and bathymetry maps are shown in Figure 13. Despite error induced by high flux flow this system maintains sub-meter accuracy.

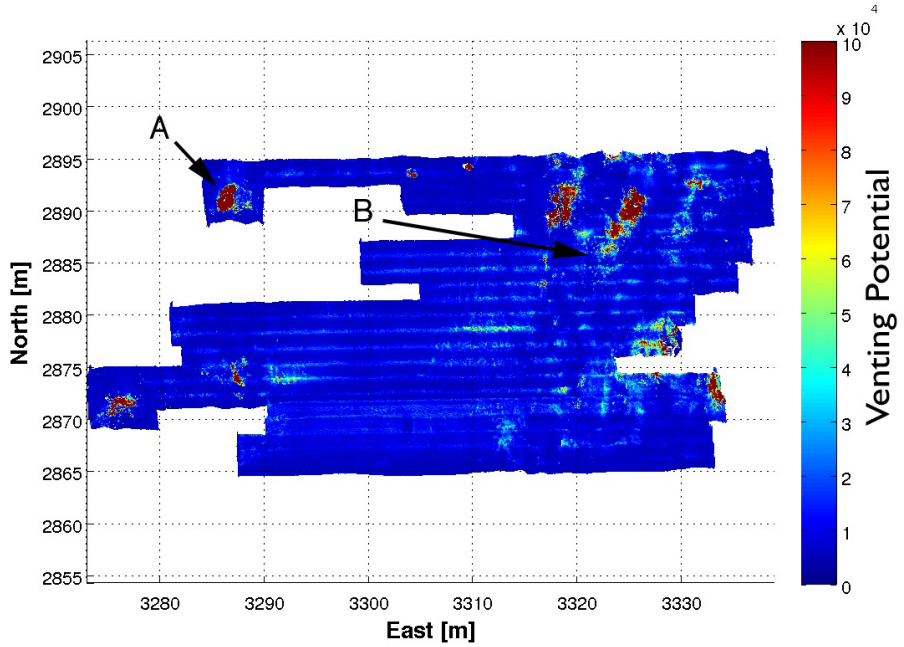

(a) Venting map

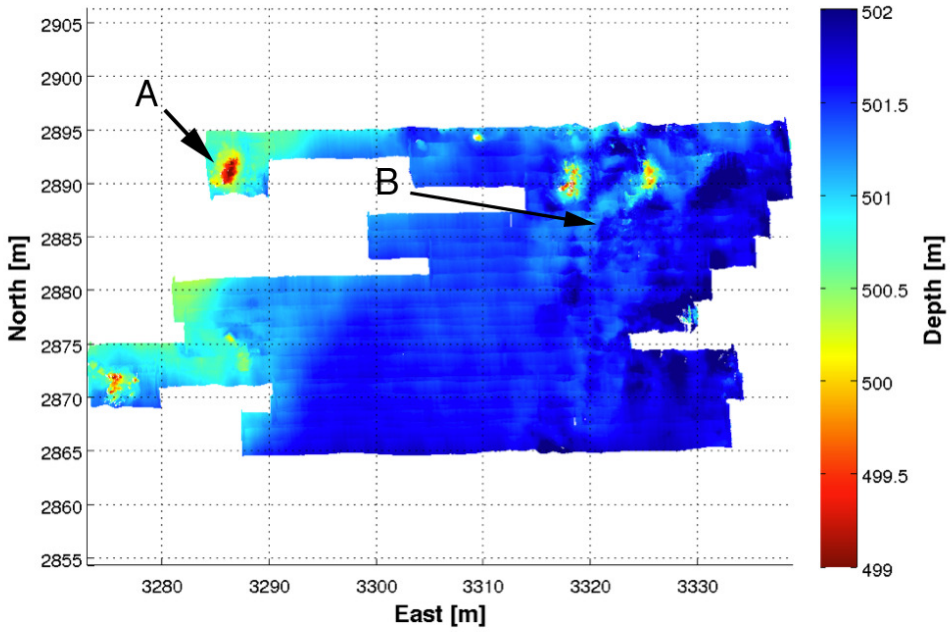

(b) Bathymetry

Figure 11: Co-located vent identification and bathymetry surveys. 11(a) A map of venting potential indicates venting at the chimney structures (labeled A) and highlights some isolated diffuse flow in areas lacking geologic features (labeled B). 11(b) The corresponding laser bathymetry of the main vent field.

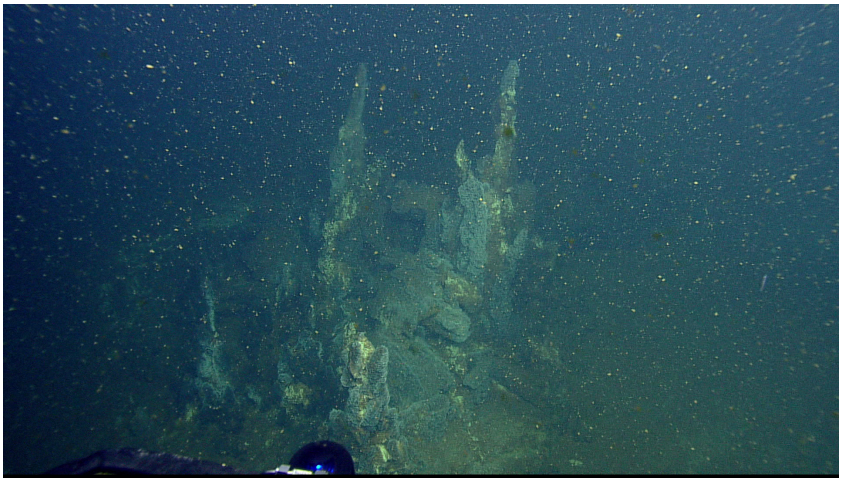

(a) Active spire vent

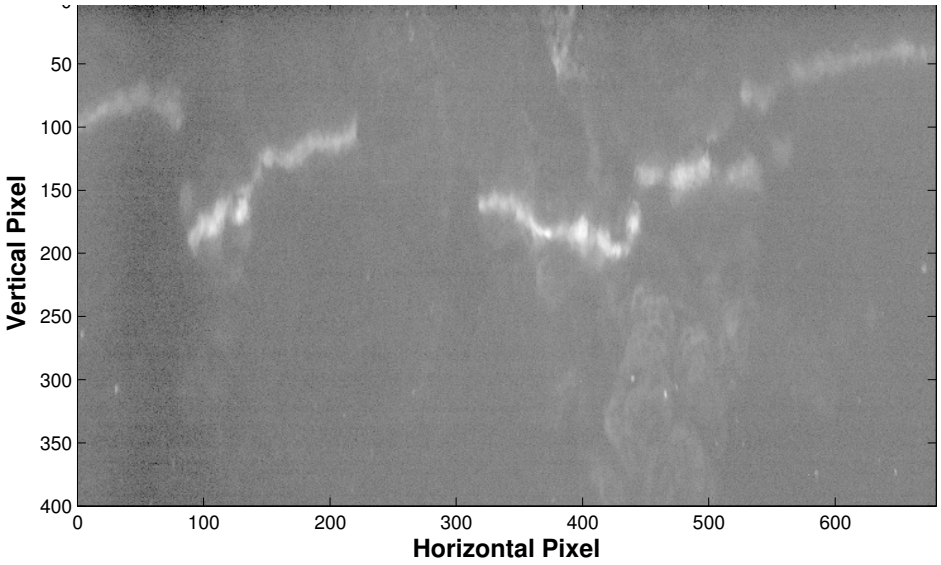

(b) Imaged laser line

Figure 12: Data collection at an active vent in the main vent field of Kolumbo Crater. 12(a) Image capture from the HD Camera mounted on *ROV Hercules* showing a mirage indicative of venting fluid. 12(b) Image of the blurred laser line passing over this vent (Logarithmic image shown for clarity)

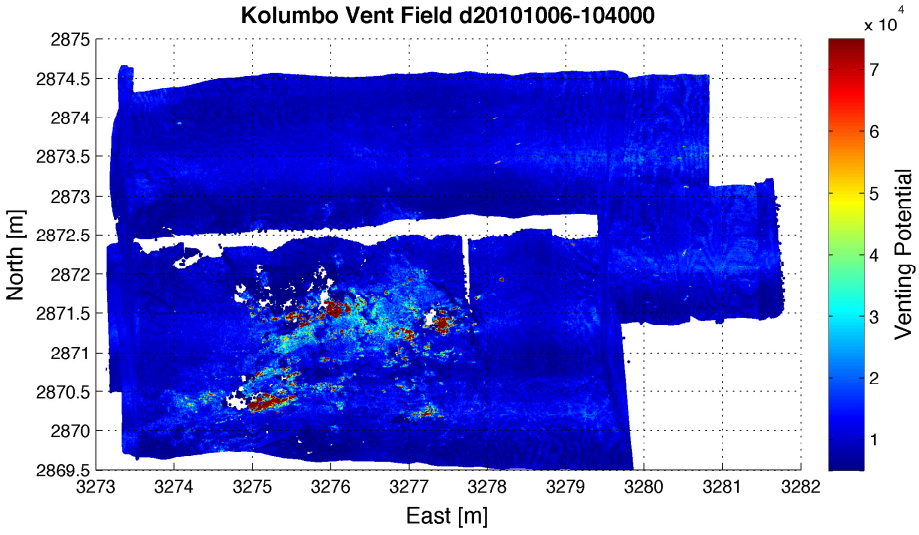

(a) Venting map

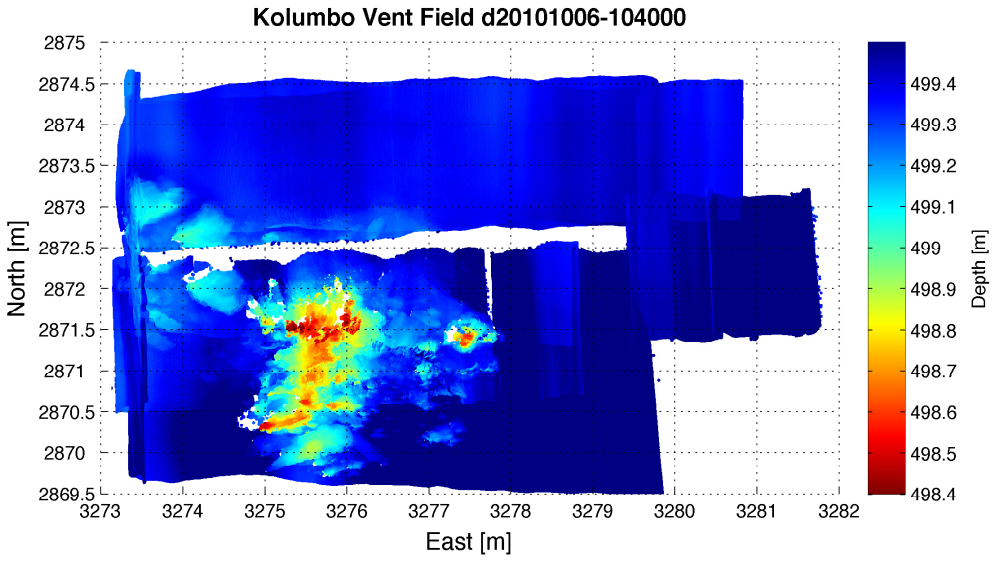

(b) Bathymetry

Figure 13: Maps of the isolated spire vent located within Kolumbo Crater. 13(a) The resulting vent map depicting localized venting at specific points within the chimney structure.13(b) High resolution laser bathymetry over the active spire vent.

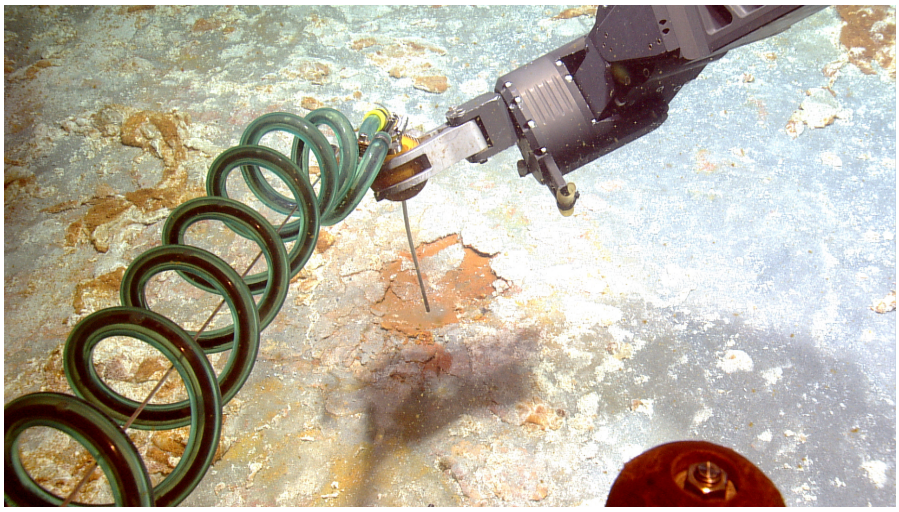

Figure 14: A temperature probe sampling at the white bacterial mats found near Poet's Candle. The brightness of the mats is apparent resulting in a high intensity return when imaged by the laser. Images from *ROV Hercules* HD camera.

1.4.2 Poets Candle, 2011

A second survey within Kolumbo encompassed an extensive area of white bacterial mats (Figure 14), indicative of diffuse sea floor venting, near the active 'Poet's Candle' vent [38]. A shimmering effect due to active venting was consistently noticeable in the HD footage centimeters above the bacterial mats, but not beyond. Temperature probes indicated a temperature range of $25 - 45°C$ above ambient, and confirmed non-homogeneous venting. Results from this survey are shown in Figure 15. The raw images from the structured light system showed only slight visible fluctuations and non-homogeneous blurring of the laser line. Comparison between an image mosaic of the area (Figure 15(a)) and the detected vent maps (Figure 15(b)) show consistencies regarding the boundaries of the bacterial mats, which are presumed be warmer than the surrounding seafloor.

In this location the highly reflective and spongy the bacterial mats may also contribute to the spread of the laser line. This issue has been noticed primarily over highly reflective bottom types which create high intensity reflections and cause the laser line to appear brighter and wider in the raw images. Additionally, in the case

of a bacteria mat the laser penetrates the material causing sub-surface reflections analogous to an internal glow. This effectively increases perceived laser line width as light scatters from within the material. Lastly, over exposure (camera boom) at the peak of the laser line due to high intensity returns can further complicate the detection process. However, even given these caveats some areas within the mat show distinctly more venting potential than others. Since the mats were observed to have a very consistent composition this confirms non-homogeneous diffuse flow.

Unlike within the main vent field, the vent activity detected within this survey can only be seen through visual inspection if the ROV is very close to the seafloor. The low temperature and low flux venting fluid disperses quickly, but as indicated by the presented maps the structured light laser system was capable of some level of remote detection of active venting.

As this data set demonstrates variations in the imaged laser line are not only influenced by changes in the refractive index but also by the seafloor. It is thus necessary to discriminate laser line distortions due to active venting from the false positives caused primarily due to bottom type characteristics. Ideally, it would be possible to isolate the flow dependent components from the background, the degree to which this is possible is still unknown.

1.4.3 Palinuro, 2011

A third data set was collected in an area of diffuse venting on the Palinuro Seamout off the coast of Italy. At a depth of approximately 600m an area of diffuse flow and biological activity, including live tubeworms, was found [41]. Active low flux venting was visually apparent at two distinct points and temperature probes reported values up to 54°C above ambient. These small diffuse vents were visually surveyed then mapped by the high resolution multibeam, the structured light laser sensor and the stereo cameras. Based on the vent map (Figure 16(b))

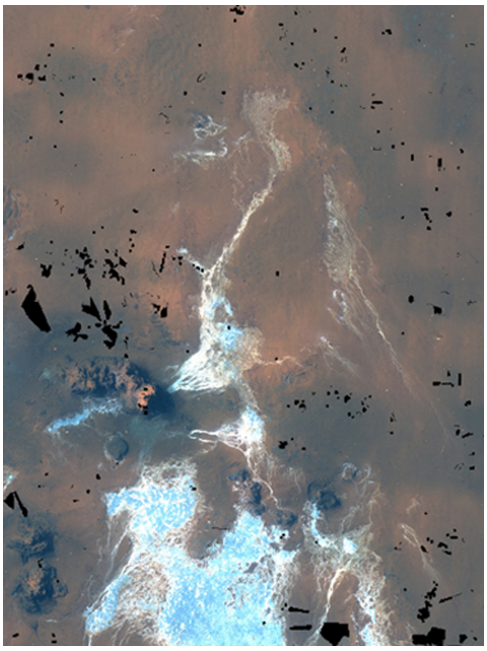

(a) Photomosaic

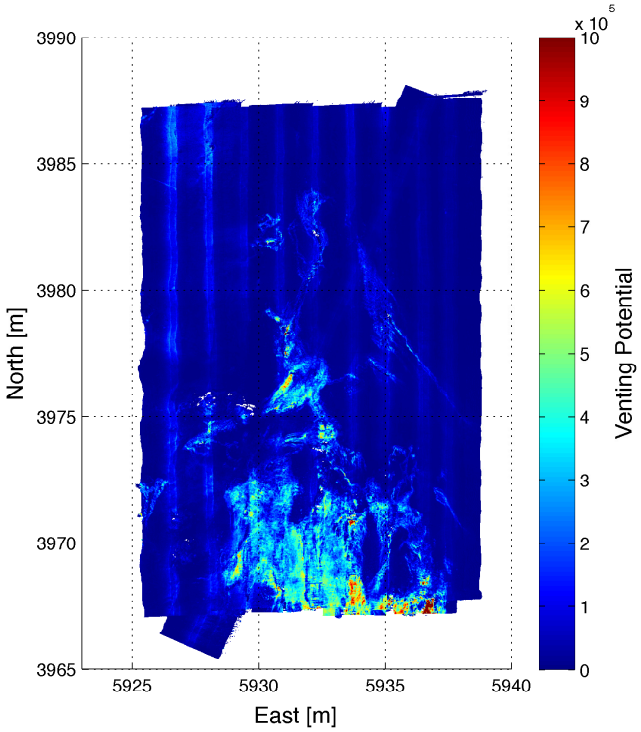

(b) Venting map

Figure 15: Maps created near the 'Poet's Candle' vent within the Kolumbo Crater. 15(a) Photomosaic showing the coverage of the white bacterial mat. 15(b) A venting potential map showing spots of higher flow (orange and red spots) and a general background patterning (light blue) consistent with the mat coverage. It is not clear if lower level signals are an artifact of the highly reflective and porous surface.

the structured light laser successfully located the two main areas of venting which correspond to rocky areas with biological activity within the image mosaic (Figure 16(a)).

MAPR

Additionally, during this survey a Miniature Autonomous Plume Recorder (MAPR) device was mounted on the ROV operating 3m above the sea floor. The MAPR, developed by NOAA's VENTS Program is a small, rugged and versatile 6000m rated sensor capable of measuring temperature, pressure and optical anomalies in an effort to collect hydrothermal plume data. The device can record temperatures with a resolution of 0.001°C and pressure to 0.2psi resolution [42].

The MAPR temperature data is plotted over the high resolution multibeam map in Figure 17. A maximum 0.15°C change in temperature was apparent. The locations of temperature anomalies do not however align with the areas of venting indicated on the vent map (Figure 16(b)) or the biological activity in the photomosaic. We attribute this to bottom currents advecting the slowly rising vent fluids. This emphasizes the value of detecting diffuse flow at the source on the sea floor. There was no temperature signal observed with the standard SeaBird 49 CTD mounted on the top of the vehicle, roughly five meters above the sea floor.

1.5 Conclusion

Systematic detection of diffuse seafloor venting can be accomplished using the vehicle (ROV or AUV) mounted structured light laser system. As the sheet laser passes through venting fluids the laser line appears blurred due to changes in the index of refraction and scattering due to turbulence. By detecting and quantifying this anomaly, a map of diffuse venting potential can be created as shown at the three vent sites presented within this paper. Although each illustrates diffuse flow

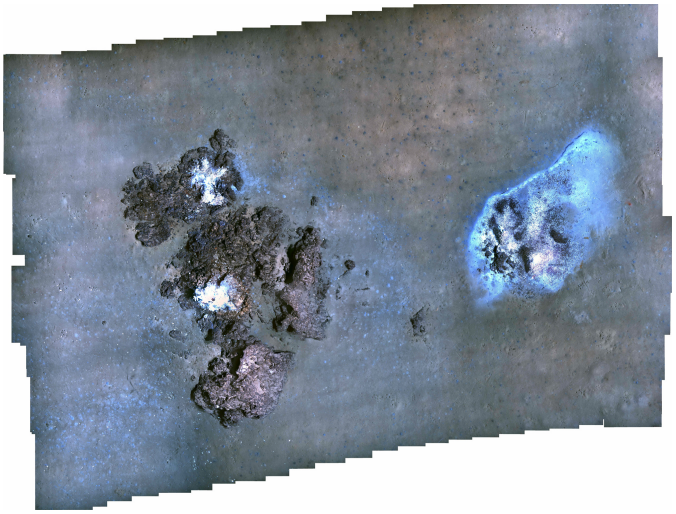

(a) Image Mosaic

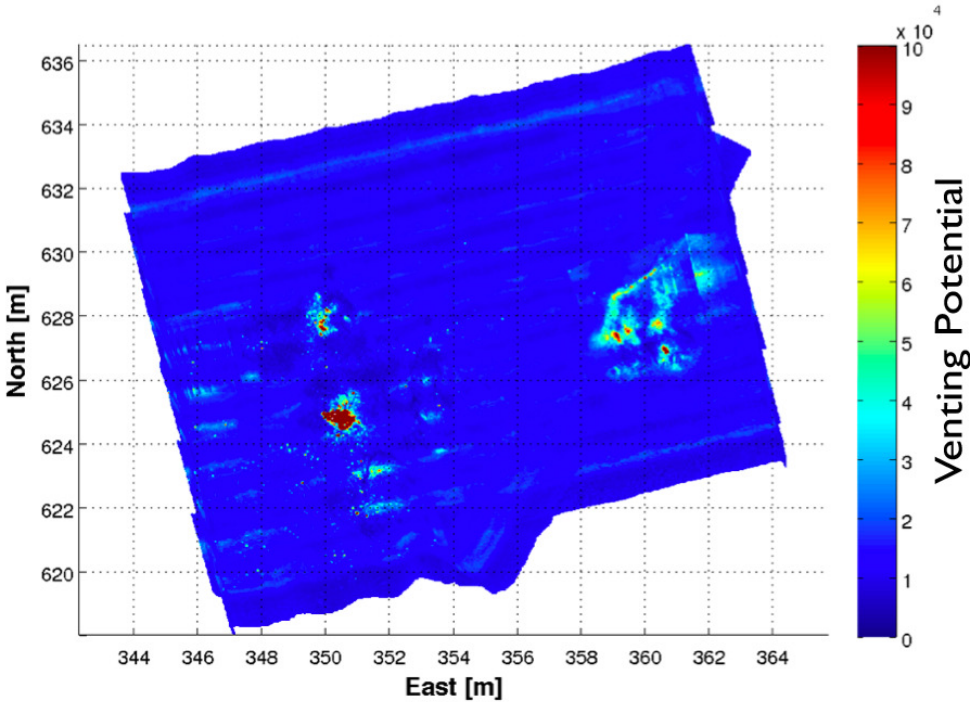

(b) Vent Map

Figure 16: Comparison between an sea floor photomosaic and the structured light map depicting areas of active venting. 16(a) Image mosaic of a geologic feature and biological activity found on the Palinuro Seamount. Living tubeworms and bacteria are indicative of areas of active diffuse venting. 16(a) The detected vent map of this same area. Distinctive areas of active venting (red) are present, primarily around areas of biological activity, however of diffuse (light blue) sea floor flow has also been detected.

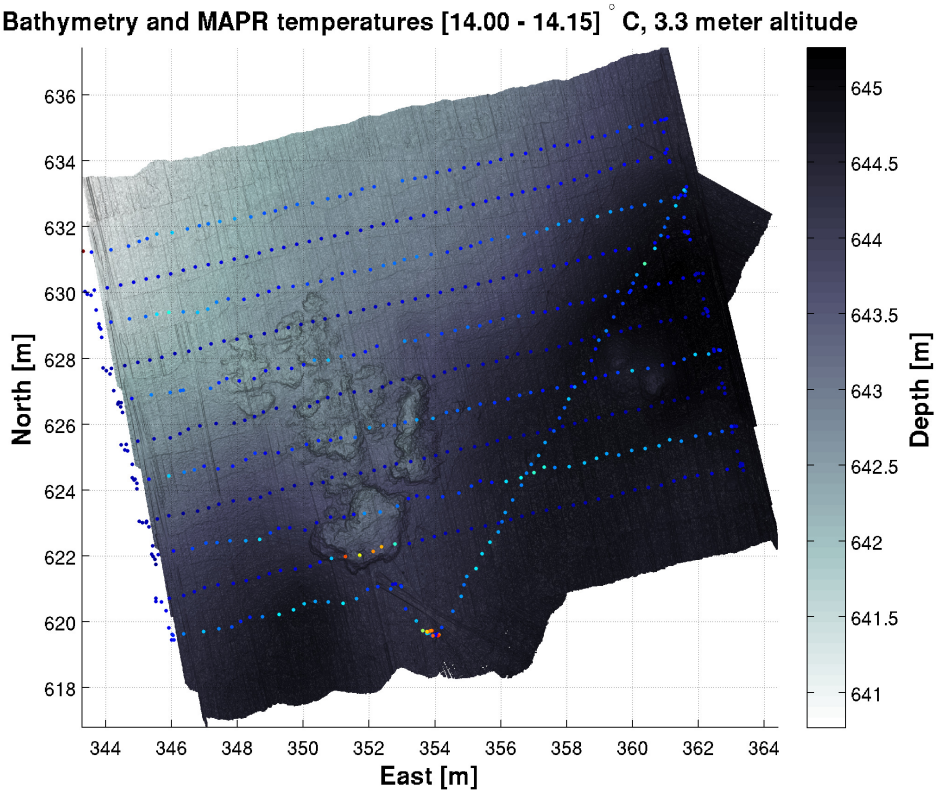

Figure 17: MAPR temperature data plotted over the multibeam bathymetric map at the Palinuro Seamount. Each colored dot represents a MAPR temperature reading where blue dots are ambient while orange and red represent a detected temperature increase. The maximum observed temperature anomaly was 0.15°C above ambient.

with unique temperature and flux characteristics the structured light laser system was capable of detection. Verification of the presence of diffuse flow has been accomplished with temperature probes and visually with a high definition camera. Future lab and field work will seek to refine the detection process isolating artifacts such as those due to bottom type characteristics. The capability to systematically detect diffuse sea floor flow and small point source vents in an autonomous fashion will allow for a comprehensive understanding of diffuse flow locations critical for interpreting its contribution to the greater ocean system.

List of References

[1] D. S. Scheirer, T. M. Shank, and D. J. Fornari, "Temperature variations at diffuse and focused flow hydrothermal vent sites along the northern East Pacific Rise," *Geochemistry Geophysics Geosystems (G3)*, vol. 7, no. 3, pp. 1525–2027, 2006.

[2] J. B. Corliss, J. Dymond, L. I. Gordon, J. M. Edmond, R. P. von Herzen, R. D. Ballard, K. Green, D. Williams, A. Bainbridge, K. Crane, and T. H. van Andel, "Submarine Thermal Springs on the Galpagos Rift," *Science*, vol. 203, pp. 1073–1083, 1979.

[3] E. Baker, G. J. Massoth, S. L. Walker, and R. W. Embley, "A method for quantitatively estimating diffuse and discrete hydrothermal discharge," *Earth and Planetary Science Letters*, vol. 118, no. 1-4, pp. 235–249, 1993.

[4] A. Schultz, P. Dickson, and H. Elderfield, "Temporal variations in diffuse hydrothermal flow at TAG," *Geophysical Research Letters*, vol. 23, no. 23, pp. 3471–3474, 1996.

[5] A. M. Pelayo, S. Stein, and C. A. Stein, "Estimation of oceanic hydrothermal heat flux from heat flow and depths of midocean ridge seismicity and magma chambers," *GRL*, vol. 21, no. 8, pp. 713–716, 1994.

[6] P. Rona and D. A. Trivett, "Discrete and diffuse heat transfer at ASHES vent field, Axial Volcano, Juan de Fuca Ridge," *Earth and Planetary Science Letters*, vol. 109, no. 1-2, pp. 57–71, 1992.

[7] A. Schultz, J. R. Delaney, and R. E. McDuff, "On the Partitioning of Heat Flux Between Diffuse and Point Source Seafloor Venting," *Journal of Geophysical Research*, vol. 97, no. B9, pp. 12 299–12 314, 1992.

[8] C. Roman, G. Inglis, and J. Rutter, "Application of structured light imaging for high resolution mapping of underwater archaeological sites," in *OCEANS 2010 IEEE - Sydney*. IEEE, May 2010, pp. 1–9.

[9] K. D. Moore, J. S. Jaffe, and B. L. Ochoa, "Development of a new underwater bathymetric laser imaging system: L-Bath," *J. Atmos. Oceanic Technol.*, vol. 17, no. 8, pp. 1106–1117, 2000.

[10] K. Moore and J. Jaffe, "Time-evolution of high-resolution topographic measurements of the sea floor using a 3-d laser line scan mapping system," *Oceanic Engineering, IEEE Journal of*, vol. 27, no. 3, pp. 525 – 545, Jul 2002.

[11] F. Bruno, G. Bianco, M. Muzzupappa, S. Barone, and A. Razionale, "Experimentation of structured light and stereo vision for underwater 3D reconstruction," *ISPRS Journal of Photogrammetry and Remote Sensing*, vol. 66, no. 4, pp. 508 – 518, 2011.

[12] S. Tetlow and J. Spours, "Three-dimensional measurement of underwater work sites using structured laser light," *Measurement Science and Technology*, vol. 10, no. 12, pp. 1162–1167, Dec. 1999.

[13] G. Inglis, C. Smart, J. Vaughn, and C. Roman, "A pipeline for structured light bathymetric mapping," in *Intelligent Robots and Systems, Proceedings. October 7-12, IEEE/RSJ International Conference on*, 2012.

[14] C. Kunz and H. Singh, "Stereo self-calibration for seafloor mapping using AUVs." IEEE, Sept. 2010, pp. 1–7. [Online]. Available: http://ieeexplore.ieee.org/xpl/freeabs_all.jsp?arnumber=5779655

[15] J.-Y. Bouguet, "Camera Calibration Toolbox for Matlab," retrieved March 2008. [Online]. Available: http://www.vision.caltech.edu/bouguetj/calib_doc/index.html

[16] C. R. German, D. R. Yoerger, M. Jakuba, T. M. Shank, C. H. Langmuir, and K. Nakamura, "Hydrothermal exploration with the Autonomous Benthic Explorer," *Deep Sea Research I*, vol. 55, no. 2, pp. 203–219, 2008.

[17] H. Singh, F. Weyer, J. Howland, A. Duester, D. Yoerger, and A. Bradley, "Quantitative stereo imaging from the Autonomous Benthic Explorer (ABE)," in *IEEE OCEANS '99*, vol. 1, 1999, pp. 52–57.

[18] T. Shank, D. Fornari, D. Yoerger, S. Humphris, and A. Bradley, "Deep Submergence Synergy: Alvin and ABE Explore the Galapagos Rift at 86 W," *EOS Transactions of the AGU*, vol. 84, no. 41, pp. 425–440, October 2003.

[19] P. Rona, "Sonar images hydrothermal vents in seafloor observatory," *EOS Transactions of the AGU*, vol. 92, no. 20, pp. 169–170, May 2011.

[20] R. Light, V. Miller, P. Rona, and K. Bemis. "Acoustic Instrumentation for Imaging and Quantifying Hydrothermal Flow in the NEPTUNE Canada Regional Cabled Observatory at Main Endeavour Field." PDF. 2012. [Online]. Available: http://www.apl.washington.edu/project/projects/covis/pdfs/COVIS_concept_operation.pdf

[21] K. C. Bell, P. Nomikou, S. Carey, E. Stathopoulou, P. Polymenakou, A. Godelitsas, C. Roman, and M. Parks, "Continued Exploration of the Santorini Volcanic Field and Cretan Basin Aegean Sea," *Oceanography*, vol. 25(1), no. supplement, 2012.

[22] R. C. Millard and G. Seaver, "An index of refraction algorithm for seawater over temperature, pressure, salinity, density, and wavelength," *Deep-Sea Research Part A*, vol. 37, no. 12, pp. 1909–1926, December 1990.

[23] H. Richard and M. Raffel, "Principle and applications of the background oriented schlieren (BOS) method," *Measurement Science and Technology*, vol. 12, pp. 1576–1585, 2001.

[24] S. B. Dalziel, G. O. Hughes, and B. R. Sutherland, "Whole-field density measurements by 'synthetic schlieren'," *Experiments in Fluids*, vol. 28, pp. 322–335, 2000.

[25] P. Rona, D. R. Jackson, T. Wen, C. Jones, K. Mitsuzawa, K. G. Bemis, and J. G. Dworski, "Acoustic mapping of diffuse flow at a seafloor hydrothermal site: Monolith Vent, Juan de Fuca Ridge," *GRL*, vol. 24, no. 19, pp. 2351–2354, 1997.

[26] D. R. Jackson and J. G. Dworski, "An acoustic backscatter thermometer for remotely mapping seafloor water temperature," *Journal of Geophysical Research: Oceans*, vol. 97(C1), pp. 761–767, 1992.

[27] J. Sarrazin, P. Rodier, M. Tivey, H. Singh, A. Schultz, and P. Sarradin, "A dual sensor device to estimate fluid flow velocity at diffuse hydrothermal vents," *Deep-Sea Research Part I: Oceanographic Research Papers*, vol. 56, no. 11, pp. 2065–2074, 2009.

[28] E. Mittelstaedt, A. Davaille, P. E. van Keken, N. Gracias, and J. Escartin, "A noninvasive method for measuring the velocity of diffuse hydrothermal flow by tracking moving refractive index anomalies," *Geochemistry Geophysics Geosystems (G3)*, vol. 11, no. 10, p. 15252027, 2010.

[29] E. Mittelstaedt, J. Escartn, N. Gracias, J. Olive, T. Barreyre, A. Davaille, M. Cannat, and R. Garcia, "Quantifying diffuse and discrete venting at the Tour Eiffel vent site, Lucky Strike hydrothermal field," *Geochemistry, Geophysics, Geosystems*, vol. 13, no. 4, pp. 1525–2027, 2012. [Online]. Available: http://dx.doi.org/10.1029/2011GC003991

[30] T. Barreyre, J. Escartn, R. Garcia, M. Cannat, E. Mittelstaedt, and R. Prados, "Structure, temporal evolution, and heat flux estimates from the Lucky Strike deep-sea hydrothermal field derived from seafloor image mosaics," *Geochemistry Geophysics Geosystems (G3)*, vol. 13, pp. 1525–2027, 2012.

[31] U. G. I. Thormahlen, J. Straub, "Index of refraction of water and its dependence on wavelength, temperature and density," *Journal of Physical Chemistry*, vol. 14, pp. 933–945, 1985.

[32] E. S. V. Karpen, L. Thomsen, "A new schlieren technique application for fluid flow visualization at cold seep sites," *Marine Geology*, vol. 204, pp. 145–159, 2004.

[33] C. D. Mobley, *Light and Water Radiative Transfer in Natural Waters*. Academic Press, 1994.

[34] G. Inglis, C. Smart, C. Roman, and S. Carey, "Detection of diffuse sea floor venting using structured light imaging," American Geophysical Union meeting, Dec 2011.

[35] J. C. Kinsey and L. L. Whitcomb, "Preliminary field experience with the dvlnav integrated navigation system for oceanographic submersibles."

[36] G. Inglis, I. Vaughn, C. Smart, and C. Roman, "Development of high resolution sea floor mapping tools and techniques," Discovery @ URI Research, Scholorship and Innovation, April 2011.

[37] C. Roman, G. Inglis, C. Smart, I. Vaughn, and S. Carey, "High resolution sea floor bathymetry using high frequency multibeam sonar and structured light laser imaging," American Geophysical Union meeting, Dec 2011.

[38] S. Carey, K. L. Croff Bell, P. Nomikou, G. Vougioukalakis, C. Roman, K. Canter, K. Bejelou, M. Bourbouli, and J. Fero Martin, "Exploration of the Kolumbo Volcanic Rift Zone," *Oceanography*, vol. 24(1), no. supplement, 2011.

[39] H. Sigurdsson, S. Carey, M. Alexandri, G. Vougioukalakis, K. Croff, and C. Roman, "Marine Investigations of Greece's Santorini Volcanic Field," *EOS Transactions of the AGU*, vol. 87, no. 34, p. 337, 2006.

[40] C. Roman, G. Inglis, J. I. Vaughn, C. Smart, B. Douillard, and S. Williams, "The development of high-resolution seafloor mapping techniques," *Oceanography*, vol. 25(1), no. supplement, 2012.

[41] S. N. Carey, K. L. C. Bell, M. Rosi, M. Marani, P. Nomikou, S. L. Walker, K. Faure, and J. Kelly, "Submarine Volcanoes of the Aeolian Arc, Tyrrhenian Sea," *Oceanography*, vol. 25(1), no. supplement, 2012.

[42] E. T. Baker and H. B. Milburn, "MAPR: A new instrument for hydrothermal plume mapping," *RIDGE Events*, vol. 8, no. 1, pp. 23–25, 1997.

BIBLIOGRAPHY

Baker, E. T. and Milburn, H. B., "MAPR: A new instrument for hydrothermal plume mapping," *RIDGE Events*, vol. 8, no. 1, pp. 23–25, 1997.

Baker, E., Massoth, G. J., Walker, S. L., and Embley, R. W., "A method for quantitatively estimating diffuse and discrete hydrothermal discharge," *Earth and Planetary Science Letters*, vol. 118, no. 1-4, pp. 235–249, 1993.

Barkby, S., W. S. B. P. O. and Jakuba, M. V., "A featureless approach to efficient bathymetric SLAM using distributed particle mapping," *Journal of Field Robotics*, 2011.

Barreyre, T., Escartn, J., Garcia, R., Cannat, M., Mittelstaedt, E., and Prados, R., "Structure, temporal evolution, and heat flux estimates from the Lucky Strike deep-sea hydrothermal field derived from seafloor image mosaics," *Geochemistry Geophysics Geosystems (G3)*, vol. 13, pp. 1525–2027, 2012.

Bell, K. C., Nomikou, P., Carey, S., Stathopoulou, E., Polymenakou, P., Godelitsas, A., Roman, C., and Parks, M., "Continued Exploration of the Santorini Volcanic Field and Cretan Basin Aegean Sea," *Oceanography*, vol. 25(1), no. supplement, 2012.

Bouguet, J.-Y., "Camera Calibration Toolbox for Matlab," retrieved March 2008. [Online]. Available: http://www.vision.caltech.edu/bouguetj/calib_doc/index.html

Bruno, F., Bianco, G., Muzzupappa, M., Barone, S., and Razionale, A., "Experimentation of structured light and stereo vision for underwater 3D reconstruction," *ISPRS Journal of Photogrammetry and Remote Sensing*, vol. 66, no. 4, pp. 508 – 518, 2011.

Carey, S., Croff Bell, K. L., Nomikou, P., Vougioukalakis, G., Roman, C., Canter, K., Bejelou, K., Bourbouli, M., and Fero Martin, J., "Exploration of the Kolumbo Volcanic Rift Zone," *Oceanography*, vol. 24(1), no. supplement, 2011.

Carey, S. N., Bell, K. L. C., Rosi, M., Marani, M., Nomikou, P., Walker, S. L., Faure, K., and Kelly, J., "Submarine Volcanoes of the Aeolian Arc, Tyrrhenian Sea," *Oceanography*, vol. 25(1), no. supplement, 2012.

Corliss, J. B., Dymond, J., Gordon, L. I., Edmond, J. M., von Herzen, R. P., Ballard, R. D., Green, K., Williams, D., Bainbridge, A., Crane, K., and van Andel, T. H., "Submarine Thermal Springs on the Galpagos Rift," *Science*, vol. 203, pp. 1073–1083, 1979.

Dalziel, S. B., Hughes, G. O., and Sutherland, B. R., "Whole-field density measurements by 'synthetic schlieren'," *Experiments in Fluids*, vol. 28, pp. 322–335, 2000.

German, C. R., Yoerger, D. R., Jakuba, M., Shank, T. M., Langmuir, C. H., and Nakamura, K., "Hydrothermal exploration with the Autonomous Benthic Explorer," *Deep Sea Research I*, vol. 55, no. 2, pp. 203–219, 2008.

I. Thormahlen, J. Straub, U. G., "Index of refraction of water and its dependence on wavelength, temperature and density," *Journal of Physical Chemistry*, vol. 14, pp. 933–945, 1985.

Inglis, G., Smart, C., Roman, C., and Carey, S., "Detection of diffuse sea floor venting using structured light imaging," American Geophysical Union meeting, Dec 2011.

Inglis, G., Smart, C., Vaughn, J., and Roman, C., "A pipeline for structured light bathymetric mapping," in *Intelligent Robots and Systems, Proceedings. October 7-12, IEEE/RSJ International Conference on*, 2012.

Inglis, G., Vaughn, I., Smart, C., and Roman, C., "Development of high resolution sea floor mapping tools and techniques," Discovery @ URI Research, Scholorship and Innovation, April 2011.

Jackson, D. R. and Dworski, J. G., "An acoustic backscatter thermometer for remotely mapping seafloor water temperature," *Journal of Geophysical Research: Oceans*, vol. 97(C1), pp. 761–767, 1992.

Kinsey, J. C. and Whitcomb, L. L., "Preliminary field experience with the dvlnav integrated navigation system for oceanographic submersibles."

Kunz, C. and Singh, H., "Stereo self-calibration for seafloor mapping using AUVs." IEEE, Sept. 2010, pp. 1–7. [Online]. Available: http://ieeexplore.ieee.org/xpl/freeabs_all.jsp?arnumber=5779655

Light, R., Miller, V., Rona, P., and Bemis, K. "Acoustic Instrumentation for Imaging and Quantifying Hydrothermal Flow in the NEPTUNE Canada Regional Cabled Observatory at Main Endeavour Field." PDF. 2012. [Online]. Available: http://www.apl.washington.edu/project/projects/covis/pdfs/COVIS_concept_operation.pdf

Millard, R. C. and Seaver, G., "An index of refraction algorithm for seawater over temperature, pressure, salinity, density, and wavelength," *Deep-Sea Research Part A*, vol. 37, no. 12, pp. 1909–1926, December 1990.

Mittelstaedt, E., Davaille, A., van Keken, P. E., Gracias, N., and Escartin, J., "A noninvasive method for measuring the velocity of diffuse hydrothermal

flow by tracking moving refractive index anomalies," *Geochemistry Geophysics Geosystems (G3)*, vol. 11, no. 10, p. 15252027, 2010.

Mittelstaedt, E., Escartn, J., Gracias, N., Olive, J., Barreyre, T., Davaille, A., Cannat, M., and Garcia, R., "Quantifying diffuse and discrete venting at the Tour Eiffel vent site, Lucky Strike hydrothermal field," *Geochemistry, Geophysics, Geosystems*, vol. 13, no. 4, pp. 1525–2027, 2012. [Online]. Available: http://dx.doi.org/10.1029/2011GC003991

Mobley, C. D., *Light and Water Radiative Transfer in Natural Waters*. Academic Press, 1994.

Moore, K. D., Jaffe, J. S., and Ochoa, B. L., "Development of a new underwater bathymetric laser imaging system: L-Bath," *J. Atmos. Oceanic Technol.*, vol. 17, no. 8, pp. 1106–1117, 2000.

Moore, K. and Jaffe, J., "Time-evolution of high-resolution topographic measurements of the sea floor using a 3-d laser line scan mapping system," *Oceanic Engineering, IEEE Journal of*, vol. 27, no. 3, pp. 525 – 545, Jul 2002.

Pelayo, A. M., Stein, S., and Stein, C. A., "Estimation of oceanic hydrothermal heat flux from heat flow and depths of midocean ridge seismicity and magma chambers," *GRL*, vol. 21, no. 8, pp. 713–716, 1994.

Richard, H. and Raffel, M., "Principle and applications of the background oriented schlieren (BOS) method," *Measurement Science and Technology*, vol. 12, pp. 1576–1585, 2001.

Roman, C., Inglis, G., and Rutter, J., "Application of structured light imaging for high resolution mapping of underwater archaeological sites," in *OCEANS 2010 IEEE - Sydney*. IEEE, May 2010, pp. 1–9.

Roman, C., Inglis, G., Smart, C., Vaughn, I., and Carey, S., "High resolution sea floor bathymetry using high frequency multibeam sonar and structured light laser imaging," American Geophysical Union meeting, Dec 2011.

Roman, C., Inglis, G., Vaughn, J. I., Smart, C., Douillard, B., and Williams, S., "The development of high-resolution seafloor mapping techniques," *Oceanography*, vol. 25(1), no. supplement, 2012.

Roman, C., Inglis, G., Vaughn, J. I., Smart, C., Douillard, B., and Williams, S., "The development of high-resolution seafloor mapping techniques," *Oceanography*, vol. 25(1), no. supplement, 2012.

Roman, C. and Singh, H., "A Self-Consistent bathymetric mapping algorithm," *Journal of Field Robotics*, vol. 24, no. 1-2, pp. 23–50, 2007.

Rona, P., "Sonar images hydrothermal vents in seafloor observatory," *EOS Transactions of the AGU*, vol. 92, no. 20, pp. 169–170, May 2011.

Rona, P. and Trivett, D. A., "Discrete and diffuse heat transfer at ASHES vent field, Axial Volcano, Juan de Fuca Ridge," *Earth and Planetary Science Letters*, vol. 109, no. 1-2, pp. 57–71, 1992.

Rona, P., Jackson, D. R., Wen, T., Jones, C., Mitsuzawa, K., Bemis, K. G., and Dworski, J. G., "Acoustic mapping of diffuse flow at a seafloor hydrothermal site: Monolith Vent, Juan de Fuca Ridge," *GRL*, vol. 24, no. 19, pp. 2351–2354, 1997.

Sarrazin, J., Rodier, P., Tivey, M., Singh, H., Schultz, A., and Sarradin, P., "A dual sensor device to estimate fluid flow velocity at diffuse hydrothermal vents," *Deep-Sea Research Part I: Oceanographic Research Papers*, vol. 56, no. 11, pp. 2065–2074, 2009.

Scheirer, D. S., Shank, T. M., and Fornari, D. J., "Temperature variations at diffuse and focused flow hydrothermal vent sites along the northern East Pacific Rise," *Geochemistry Geophysics Geosystems (G3)*, vol. 7, no. 3, pp. 1525–2027, 2006.

Schultz, A., Delaney, J. R., and McDuff, R. E., "On the Partitioning of Heat Flux Between Diffuse and Point Source Seafloor Venting," *Journal of Geophysical Research*, vol. 97, no. B9, pp. 12 299–12 314, 1992.

Schultz, A., Dickson, P., and Elderfield, H., "Temporal variations in diffuse hydrothermal flow at TAG," *Geophysical Research Letters*, vol. 23, no. 23, pp. 3471–3474, 1996.

Shank, T., Fornari, D., Yoerger, D., Humphris, S., and Bradley, A., "Deep Submergence Synergy: Alvin and ABE Explore the Galapagos Rift at 86 W," *EOS Transactions of the AGU*, vol. 84, no. 41, pp. 425–440, October 2003.

Sigurdsson, H., Carey, S., Alexandri, M., Vougioukalakis, G., Croff, K., and Roman, C., "Marine Investigations of Greece's Santorini Volcanic Field," *EOS Transactions of the AGU*, vol. 87, no. 34, p. 337, 2006.

Singh, H., Weyer, F., Howland, J., Duester, A., Yoerger, D., and Bradley, A., "Quantitative stereo imaging from the Autonomous Benthic Explorer (ABE)," in *IEEE OCEANS '99*, vol. 1, 1999, pp. 52–57.

Tetlow, S. and Spours, J., "Three-dimensional measurement of underwater work sites using structured laser light," *Measurement Science and Technology*, vol. 10, no. 12, pp. 1162–1167, Dec. 1999.

V. Karpen, L. Thomsen, E. S., "A new schlieren technique application for fluid flow visualization at cold seep sites," *Marine Geology*, vol. 204, pp. 145–159, 2004.

Vaughn, J. I., "Self-consistent microbathymetry from high resolution sensors and self-contained navigation," Master's thesis, University of Rhode Island, 2012.